OVERVIEW OF RECENT TRENDS AND DEVELOPMENTS FOR BPM SYSTEMS*

M. Wendt#, Fermilab, Batavia, IL 60510, U.S.A.

Abstract

Beam position monitoring (BPM) systems are the workhorse of beam diagnostics for almost any kind of charged particle accelerator: linear, circular or transport-lines, operating with leptons, hadrons or heavy ions. BPMs are essential for beam commissioning, accelerator fault analysis and trouble shooting, machine optics, as well as lattice measurements, and finally, for accelerator optimization, in order to achieve the ultimate beam quality.

This presentation summarizes the efforts of the beam instrumentation community on recent developments and advances on BPM technologies, i.e. BPM pickup monitors and front-end electronics (analog and digital). Principles, examples, and state-of-the-art status on various BPM techniques, serving hadron and heavy ion machines, sync light synchrotron's, as well as electron linacs for FEL or HEP applications are outlined.

INTRODUCTION

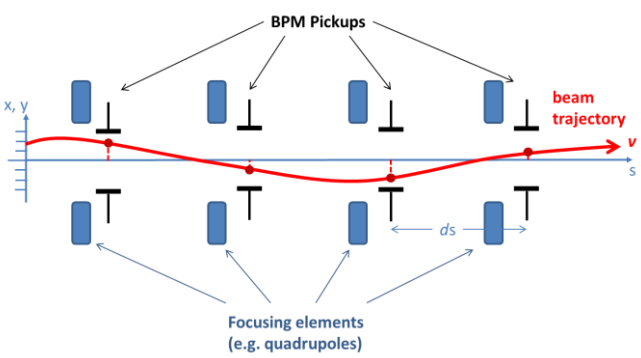

Figure 1: Measurement of the beam trajectory.

The observation of the beam trajectory

$$u(s) = A\sqrt{\beta}\sin(Q\varphi + \delta) \qquad (1)$$

with $u = (x, y)$ as the transverse coordinates, A the amplitude of the oscillation, β the beta-function, Q the betatron tune, $\varphi = 0\ldots2\pi$, and δ an initial condition, is one of the most fundamental beam measurements in any particle accelerator. A series of beam position monitors (BPM) are distributed along the beam-line, preferably near the focusing elements (e.g. quadrupole magnets), see Figure 1. The BPMs monitor the transverse beam displacement (x, y) at their locations s_n, knowing the distance ds between two monitors we may also get the slope (x', y') of the beam trajectory – if no optical elements are in-between.

* This work was supported by Fermi National Accelerator Laboratory, operated by Fermi Research Alliance, LLC under contract No. DE-AC02-07CH11359 with the United States Department of Energy
#manfred@fnal.gov

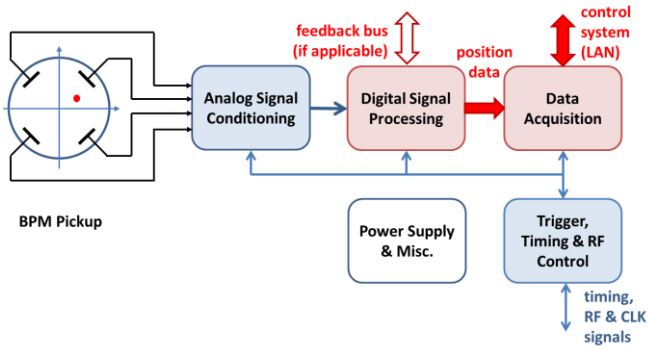

Figure 2: Schematics of a beam position monitor.

Each beam position monitor consists of a BPM pickup, with two or four symmetrically arranged electrodes, followed by a readout electronics system for signal conditioning and processing (Fig. 2). The pickup electrodes sense a part of the electromagnetic field of the passing beam and convert it to an electrical signal. The read-out electronics extract the beam position information out of the electrode signals by conditioning the analog signal, followed by digital signal processing techniques. The position data and other controls of the BPM read-out system are handled by a data acquisition interface, typically a CPU processor, which interfaces to the accelerator control system. The digital signal processing and data acquisition has to be supported by timing and clock signals, which are also used for time stamping, i.e. synchronizing BPM data across the entire system, as well as accelerator event and RF signals (for analog signal conditioning).

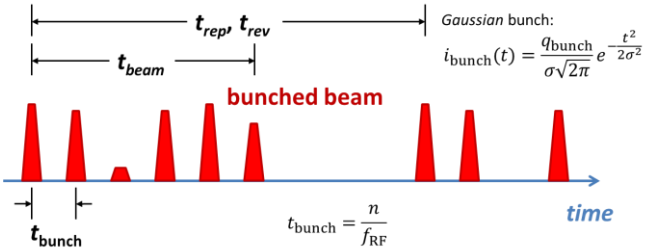

Figure 3: Beam structure.

The particle beam is a bunched stimulus signal for the BPM, with $t_{\mathrm{bunch}} = n/f_{\mathrm{RF}}$. As Figure 3 indicates, the beam bunches may have different intensities, sometimes even missing bunches. The beam structure spans t_{beam}, and typically repeats with t_{rep} in linacs and transport-lines, and t_{rev} in circular accelerators. Depending on the measurement or integration time of the BPM, we can resolve the beam position of single or all individual bunches, or the average over one or several beam pulses

or turns. Multipurpose accelerators, such as the CERN PS or the Fermilab Main Injector may accelerate different beam structures, apply sophisticated RF gymnastics and even use different particle species, which further complicates the operating conditions for the BPM system [1].

Some important characteristics of a BPM system are:

- *Measurement / integration time*, as described.
- *Position resolution*, i.e. the minimum beam displacement difference the BPM can resolve (typically depends a lot on the integration time).
- *Linearity and accuracy*, i.e. the absolute error of the reported beam position, over a part or the complete range of the beam pipe aperture.
- *x-y coupling*
- *Dynamic range*, in terms of beam intensity. The reported beam position has to be independent of the beam intensity, saturation or noise effects will appear at high / low beam intensities and compromise linearity and position resolution.
- *Reproducibility and long term stability* are important for storage rings and beam lattices which critically rely on references orbits.

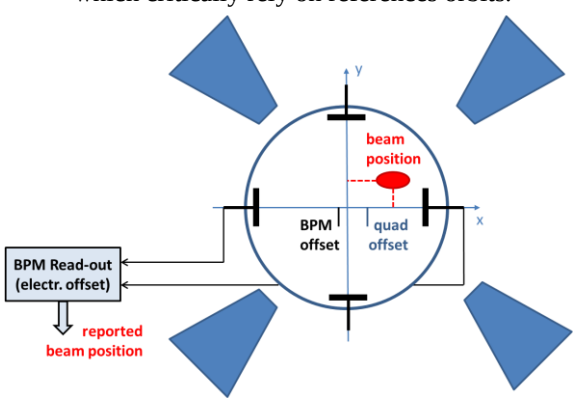

Figure 4: BPM and quadrupole offsets.

The zero-order effect of the linearity correction is the so-called *BPM-offset*. Fig. 4 illustrates the BPM and quadrupole offsets with respect to the vacuum pipe. A beam-based alignment (BBA) procedure can be performed to characterize the BPM-to-quadrupole offset and tilt, including the effects of the electronics [2], [3]. [4].

Digital signal processing allows us to simultaneously output BPM data with different integration times, e.g. multiturn averaged position data, single pass / turn-by-turn, or even single bunch displacement information. This enables besides the beam orbit characterization, a large variety of direct and indirect beam measurements and observations, e.g. injection oscillations, betatron and synchrotron tunes, dispersion and beam energy, x-y coupling, beam optics, magnet alignment and errors, non-linear field effects, etc. [5]. For machine commissioning the processing of the beam intensity signal is of great value, while precise, RF derived clock signals also enable beam phase and time-of-flight measurements with today's BPM systems.

BPM PICKUP

The BPM pickup is an arrangement of electromagnetic antennas or a resonant device, and part of the accelerator vacuum system. In a simplistic view, for relativistic beams ($v \approx c_0$), the output signal of a BPM pickup can be expressed:

$$V_{\text{elec}}(x,y,\omega) = s(x,y)\,Z(\omega)\,I_{\text{beam}}(\omega) \qquad (2a)$$

$$V_{\Delta}(x,y,\omega) = s(x,y,\omega)\,Z(\omega)\,I_{\text{beam}}(\omega) \qquad (2b)$$

where V is the output signal for a broadband pickup electrode (2a) or a resonant cavity (2b), $Z(\omega)$ is the frequency dependent transfer function or shunt impedance of the pickup, and $s(x,y,\omega)$ is sensitive to the beam position (x,y), and eventually also frequency dependent. The beam current $I_{\text{beam}}(\omega)$ can often be approximated by a Gaussian function for the bunch signal, with a repetition similar as shown in Fig. 3. Most BPM pickups can be classified as either broadband or resonant. Besides being an RF or microwave device, the BPM pickup has to be UHV certified, and in some superconducting cryogenic installations also must operate at cryogenic temperatures and meet special cleanroom requirements.

Broadband BPM Pickups

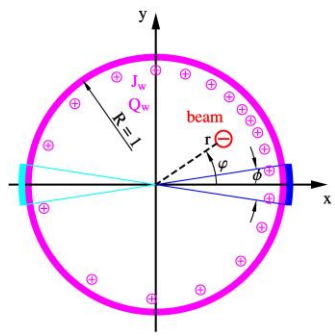

Figure 5: Beam and image currents.

For a broadband BPM pickup the sensitivity s in eq. (2a) is independent of ω. Broadband BPMs operate in terms of the image current model (Fig. 5), this *Laplace* problem was solved analytically for a beam pipe with circular or elliptical cross-section [6], [7], [8]:

$$J_{\text{w}}(R=1,\phi_w) = I_0 \frac{1-\rho^2}{1+\rho^2-2\rho\cos(\phi_w-\varphi)} \qquad (3)$$

Eq. (3) returns the image current density J_{w} at the surface of the beam pipe (R=1, ϕ_w) for a beam position at ($\rho=r/R$, φ), where $I_0=I_{\text{beam}}/2\pi$. Integrating ϕ_w over the range of the BPM electrode ϕ gives the electrode current I_{elec}, for which the geometric part is (note: cylindrical coordinates)

$$s(\rho,\varphi) = \phi + 4\sum_{n=1}^{\infty}\frac{\rho^n}{n}\cos(n\varphi)\sin\left(\frac{n\phi}{2}\right) \qquad (4)$$

Two symmetric arranged electrodes A, B (e.g. horizontal, as in Fig. 5) can now perform as BPM:

$$\text{beam pos.} = f\left(\frac{A-B}{A+B}\right) \text{ or } = f\left(20\log_{10}\left(\frac{A}{B}\right)\right) \qquad (5)$$

With typical pickup dimensions, e.g. R=25 mm, $\phi=30^0$, the sensitivity computes to 2.75 dB/mm around the beam pipe center. As eq. (2a) indicates, all broadband BPMs, suffer from a strong I_{beam} common mode term in the output signal, with a small amplitude modulation component due to the beam position *(x,y)*. The position sensitivity is basically fixed by the geometry and the related image current distribution, eq. (3), (4), (5).

Most prominent and widely applied member of the broadband BPM family is the electrostatic (capacitive) coupling so-called "button BPM" (different commercial button BPM feedthroughs are available). Also the stripline BPM (electromagnetic coupling) is popular, the length of the striplines, allows to match $Z(\omega)$ to the bunch spectrum $I_{bunch}(\omega)$. Circular split-plane ("shoe-box") BPMs have an almost linear position dependence, which also can be achieved with large capacitive electrodes, spanning $\phi \approx 60^0$. [9] uses BPMs with magnetic coupling loop antennas for beam position monitoring near the dump, and [10] gives further theoretical background on magnetic BPMs, also for detection of the beam angle. [11] developed a inductive BPM with single pass capability and sub-micrometer resolution.

While all broadband BPMs basically follow with their position characteristics the image current model, they differ in their frequency behavior $Z(\omega)$, which is discussed extensively [12], [13], [14]. The numerical solution of the Laplace equation allows a more precise approach to evaluate *s(x,y)*, also for non-circular cross-sections of the beam pipe. The results can be fitted with 2-D polynomials or look-up tables, allowing a linearization in the post-processing of the BPM data.

The effect of non-relativistic beams to the sensitivity of different BPM electrode shapes has been studied in great detail with help of numerical methods [15].

Resonant BPM Pickups

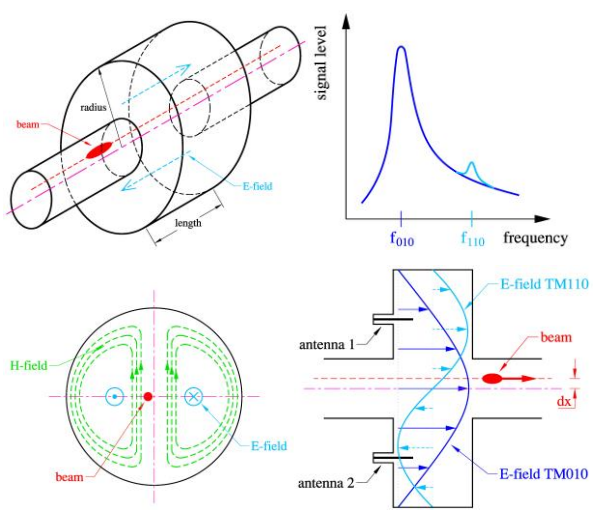

Figure 6: "Pillbox" cavity as BPM.

A cylindrical "pillbox" with conductive walls of length ℓ and radius R resonates at its eigenfrequencies

$$f_{mnp} = \frac{1}{2\pi\sqrt{\mu_0 \varepsilon_0}} \sqrt{\left(\frac{j_{mn}}{R}\right)^2 + \left(\frac{p\pi}{\ell}\right)^2} \qquad (6)$$

This resonator can be utilized as passive, beam driven cavity BPM by providing beam pipe ports (Fig. 6). A subset of the eigenmodes eq. (6) is excited by the bunched beam, for the application as BPM the lowest transverse-magnetic dipole mode TM_{110} is of interest. Its

$$E_z = C\, J_1\left(\frac{j_{11} r}{R}\right) e^{i\omega t} \cos\varphi \qquad (7)$$

field component couples to the beam with an almost linear dependence to the beam displacement *r*, and vanishes when the beam is in the center ($r = 0$). Four symmetrically arranged pin antenna feedthroughs fix the polarization of TM_{110} to the horizontal and vertical axis, and provide the unnormalized difference signal $\Delta = f(x,y,I_{beam})$, the beam intensity is hidden in the constant *C*.

Resonant structures, e.g. "pill-box" or rectangular cavities, also coaxial resonators, and more complex waveguide-loaded resonators, became very popular to fulfil the high resolution, single-pass beam position monitoring demands of linear accelerators for the high luminosity final focus lattice [16], [17], or driving a SASE-FEL beam-line [18]. In [19] the operation of a simple cavity BPM inside a cryostat is presented. The discussion on the theoretical background was recently updated [20]. The x-y decoupling of the TM_{110} polarization is addressed in [21]. The high resolution potential of a BPM system with C-Band choke-mode resonators was demonstrated the first time at the SLAC final focus test beam, achieving 25 nm single-bunch, single-pass position resolution [22].

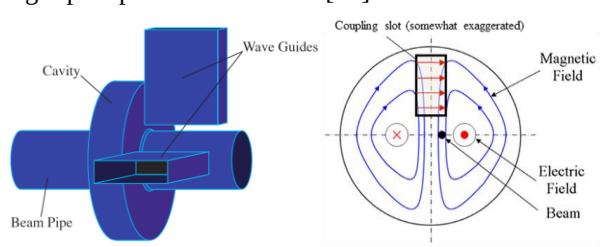

Figure 7: Waveguide-loaded cavity BPM.

The presence of the fundamental TM_{010} monopole mode adds a strong common mode component to the dipole-mode position signal, and even having a different frequency f_{010}, it limits the performance of the cavity BPM. A waveguide of width *a*, with a cut-off frequency

$$f_{010} < f_{10} = \frac{1}{2a\sqrt{\mu\varepsilon}} < f_{110} \qquad (8)$$

acts as very efficient, internal high-pass filter, and makes the cavity BPM quasi "common-mode free" (Fig. 7). The coupling slot between resonator and waveguide also helps to align the TM_{110} polarization planes, and minimizes the x-y coupling. However, the finite Q-value of the resonances still causes an unwanted leakage of the

monopole-mode at the frequency f_{110} of the dipole mode, thus limiting the resolution.

The first test of a system of three waveguide-loaded 14 GHz cavity BPMs was performed at BNL, demonstrating 150 nm beam position resolution [23]. Separate waveguide-loaded rectangular resonators (Fig. 8), operating at different C-Band frequencies achieved 8.7 nm resolution at the ATF2 final focus test beam-line [24].

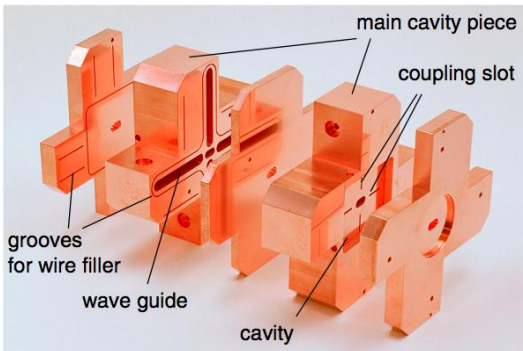

Figure 8: The ATF2 IP-BPM.

A magnetic waveguide-to-coaxial port coupling was introduced for the C-Band cavity BPMs at SPring-8 [25], a similar construction is tested for the XFEL [26]. The monopole-mode (TM_{010}) reference resonator, required to deliver beam intensity and phase reference signals to the read-out electronics, is also used as beam arrival time monitor, showing a 25 fsec temporal resolution performance. A low-Q, mass-producible X-Band cavity BPM for the CLIC main linac is under development, targeting <50 nm spatial resolution at <50 nsec integration time. Details on the effects of tolerances are discussed, as well as performance limitations due to mode leaking, and a comparison between single vs. multi-bunch beam stimulus [27].

Beam position monitoring based on TEM coaxial resonators, the so-called re-entrant cavity BPM, has also been studied, and is proposed to operate inside the cryomodule at the European XFEL project [28]. A waveguide-loaded version demonstrated sub-micron resolution, when tested under single-bunch, single-pass beam conditions [29].

Beam excited dipole mode signals from the HOM-couplers of standing wave accelerating structures have been studied at the FLASH FEL facility. An online SVD algorithm was used to orthogonalize the signals, thus make HOM signals usable as beam position monitor [30].

READ-OUT ELECTRONICS

The read-out system interfaces the BPM pickup to the accelerator data acquisition (control) system (Fig. 2). Signal conditioning, normalization and linearization of the position signals / data have to be provided for the time stamped beam position data. To achieve long term stability, calibration signals for gain-correction, or other correction methods are added to the system. The BPM data may also serve in beam orbit feedback systems, thus a low latency of the signal processing is of important value.

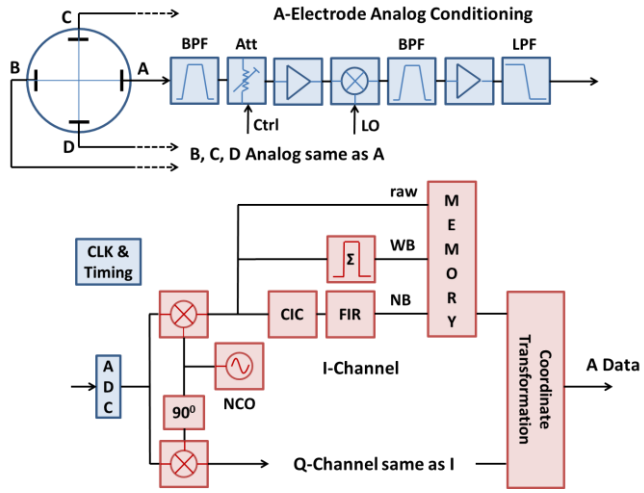

Figure 9: Key elements of the BPM read-out electronics.

An overview of "traditional" BPM read-out techniques was summarized in [31]. Today the BPM read-out electronics is typically based on frequency domain signal processing techniques, which were developed for the telecommunications market [32]. Bandpass filters in the analog section prepare the BPM pickup signals into sinewave-like burst signals, for waveform singal sampling and processing in the digital section. Microwave and RF analog components, 12-16 bit pipeline ADCs, FPGAs and clock distribution chips with sub-psec jitter are some of the key hardware elements. Figure 9 illustrates a typical electronics arrangement for a broad-band BPM pickup, 1-of-4 channels is shown. In some cases the analog down-mixer can be omitted, for cavity BPMs the schematics is similar, here the analog mixer is still required. The digital signal processing takes place in a FPGA, the I-Q down-conversion to baseband is required if the ADC clock is not locked to the accelerator RF.

As Figure 9 indicates, the measurement of the pickup electrodes signals (A, B, C, and D) is performed separately, normalization and linearization takes place in the FPGA or CPU. Drifts and aging effects have to be compensated by a calibration tone signal [33], or a channel switching scheme [34]. The effect of ADC clock jitter is discussed in various application notes [35], this becomes particulary critical in systems with heavy undersampling ($f_{signal} >> f_{CLK}$). The digital data stream can be filtered and decimated in various ways, Fig. 8 indicates how narrow-band, wide-band and raw signals can be handled simultaneously. We usually down-convert f_{signal}-f_{NCO} not exactly to DC, but to a low frequency with an integer number of oscillations over the measurement period, this avoids a crawling phase.

ACKNOWLEGEMENTS

Thanks to all the colleagues of the beam instrumentation community for their great help and support in preparing this document!

REFERENCES

[1] B. Banerjee, et.al., "Fermilab Main Injector Beam Position Monitor Upgrade," BIW'06, Batavia, IL, USA, May 2006, AIP Conf. Proc. **868** (2006), pp. 540-548.

[2] R. Brinkmann and M. Boege, "Beam-Based Alignment and Polarization Optimization in the HERA Electron Ring," EPAC'94, London, UK, June/July 1994, pp. 938-940.

[3] C. E. Adolphsen, et.al., "Beam-Based Alignment Technique for the SLC Linac," PAC'89, Chicago, IL, USA, March 1989, Proc. of IEEE (1998), SLAC-PUB-4902

[4] M. Boege, et.al., "The Swiss Light Source A "Test-Bed" for Damping Ring Optimization," IPAC'10, Kyoto, Japan, May 2010, WEPE091, pp. 3560-62 (2010).

[5] A. Hofmann, "Beam Diagnostics and Applications," BIW'98, Stanford, CA, USA, May 1998, AIP Conf. Proc. **451** (1998), pp. 3-22.

[6] J. Cuperus, "Monitoring of Particle Beams at High Frequencies," CERN, Geneva, Switzerland, November 1976, CERN/PS/LIN 76-7.

[7] K. Satoh, "New Beam Position Monitor by detecting Wall Currents," Rev. Sci. Instr. **4** (1979), p. 450.

[8] R. C. Shafer, "Characteristics of Directional Coupler Beam Position Monitors," PAC'85, Vancouver, BC, Canada, May 1985, IEEE Trans. Nucl. Sci. **32** (1985), pp. 1933-37.

[9] N. Baboi, et.al., "Magnetic Coupled Beam Position Monitor for the FLASH Dump Line," BIW'10, Santa Fe, NM, USA, May 2010, TUPSM039, pp. 214-217 (2010).

[10] X. He, et.al., "Direct Measurement of the Beam Deflection Angle using the axial B-dot Field," APS Phys. Rev. 2011, to be published

[11] I. Podadera, et.al., "Precision Beam Position Monitor for EUROTeV," DIPAC'07, Venice, Italy, May 2007, TUPB03, pp. 57-59 (2007).

[12] R. C. Shafer, "Beam Position Monitoring," BIW'89, Uptown, NY, USA, October 1989, AIP Conf. Proc. **212** (1989), pp. 26-58.

[13] D. P. McGinnis, "The Design of Beam Pickup and Kickers," BIW'94, Vancouver, BC, Canada, October 1994, AIP Conf. Proc. **333** (1994), pp. 64-85.

[14] F. Marcellini, et.al., "DAΦNE Broad-Band Button Electrodes," INFN-LNF Frascati, January 16, 1996, Note: **CD-6**.

[15] P. Kowina, et.al., "FEM Simulations – A Powerful Tool for BPM Design," DIPAC'09, Basel, Switzerland, May 2009, MOOC03, pp. 35-37 (2009).

[16] S. Walson, et.al., "Performance of a High Resolution Cavity Beam Position Monitor System," NIM-A, **578** (2007), pp. 1-22.

[17] S. T. Boogert, et.al., "Cavity Beam Position Monitor System for ATF2," IPAC'10, Kyoto, Japan, May 2010, MOPE070, pp. 1140-42 (2010).

[18] S. Smith, et.al., "LCLS Cavity Beam Position Monitors," DIPAC'09, Basel, Switzerland, May 2009, TUOC03, pp. 285-287 (2009).

[19] R. Lorenz, "Cavity Beam Position Monitors," BIW'98, Stanford, CA, USA, May 1998, AIP Conf. Proc. **451** (1998), pp. 53-73.

[20] D. Lipka, et.al., "Cavity BPM Designs, Related Electronics and Measured Performances," DIPAC'09, Basel, Switzerland, May 2009, MOPD07, pp. 280-284 (2009).

[21] V. Sargsyan, "Cavity Beam Position Monitor for the TESLA Cryomodule – Cross-Talk Minimization," Ph. D. thesis, Technical University Berlin, Germany (2003).

[22] T. Slaton, et.al., "Development of Nanometer Resolution C-Band Radio Frequency Beam Position Monitors in the Final Focus Test Beam," SLAC-PUB-7921, August 1998

[23] V. Balakin, et.al., "Experimental Results form a Microwave Cavity Beam Position Monitor," PAC'99, New York, NY, USA, March/April 1999, IEEE Proc. (1999), pp. 461-464.

[24] T. Nakamura, et.al., "High Resolution Cavity BPM for ILC Final Focus System (IP-BPM)," LCWS/ILC 2007, Hamburg, Germany, May/June 2007, arXiv:0709.2254v1, eConf C0705302.

[25] H. Maesaka, et.al., "Development of the RF Cavity BPM of XFEL/Spring-8," DIPAC'09, Basel, Switzerland, May 2009, MOPD07, pp. 56-58 (2009).

[26] D. Lipka, et.al., "Orthogonal Coupling in Cavity BPM with Slots," DIPAC'09, Basel, Switzerland, May 2009, MOPD07, pp. 44-46 (2009).

[27] H. Schmickler, et.al., "Submicron Mulit-Bunch BPM for CLIC," IPAC'10, Kyoto, Japan, May 2010, MOPE087, pp. 1185-87 (2010).

[28] C. Simon, et.al., "Status of the Re-entrant Cavity Beam Position Monitor for the European XFEL Project," BIW'10, Santa Fe, NM, USA, May 2010, TUPSM038, pp. 210-213 (2010).

[29] J. Y. Ryu, et.al., "Development of a Re-entrant Cavity L-Band Beam Position Monitor for ILC," to be published.

[30] S. Molloy, et.al., "High Precision Superconducting Cavity Diangostics with Higher Order Mode Measurements," Phys. Rev. ST Accel. Beams **9**, 112802 (2006).

[31] G. Vismara, "Signal Processing for Beam Position Monitors," BIW'00, Cambridge, MA, USA, May 2000, AIP Conf. Proc. **546** (2000), pp. 36-60.

[32] V. Schlott, et.al., "First Operational Experience with the Digital Beam Position Monitoring System for the Swiss Light Source," EPAC'00, Vienna, Austria, June 2000, pp. 1809-11.

[33] M. Wendt, et.al., "High Resolution BPMs with Integrated Gain Correction System," DIPAC'09, Basel, Switzerland, May 2009, MOPD19, pp. 89-91 (2009).

[34] Instrumentation Technologies, http://www.i-tech.si

[35] Analog Devices, AN-282, AN-501.